International Journal of Engineering & Applied Sciences (IJEAS)
Vol.17, Issue 3 (1647694) 131-140
http://dx.doi.org/10.24107/ijeas.1647694
Int J Eng Appl Sci 17(3) (2025) 131-140

The Numerical Simulation of Two-Phase Sloshing in Fluid Tanks Using VoF Method

Fuat Tan [a], Hamid Orhun Tur [b]*

Balikesir University, Department of Mechanical Engineering

fuattan@balikesir.edu.tr[a*] :000-0002-4194-5591 [*a], 0009-0005-7850-6372 [b]

Received: 26.02.2025, Revised: 01.05.2025, Accepted: 05.05.2025

Abstract

The present research was focused on modeling the sloshing of a liquid in a rectangular tank with varying heights of kerosene-air and water-air mixtures using the Volume of Fluid (VoF) model. The study's goal was to analyze the influence of the fluid type and fill level on dynamic pressure and turbulence kinetic energy in the tank. Two different fill levels (50% and 75%) were used and the outcomes for kerosene-air and water-air mixtures were compared. The results showed that models with kerosene generated larger dynamic pressure and higher turbulence kinetic energies as compared to water-filled ones. In the 75% case of kerosene, the highest dynamic pressure was about 2.3 kPa, whilst the pressure in the water-filled model was lower. A similar pattern was evident for turbulence kinetic energy, as the levels in models with kerosene were much bigger. This difference is attributed to the higher viscosity of kerosene, which creates greater resistance during sloshing. Overall, the study demonstrates that fluid type, viscosity, and fill level are the key factors in sloshing dynamics and must be prioritized in tank design.

Keywords: Dynamic pressure, Sloshing Tank, Turbulence kinetic energy, VoF

1. Introduction

Sloshing in containers exposed to external forces is particularly important during the transport of flammable and hazardous materials [1]. Sloshing has been widely studied in ocean and civil engineering [2–3]. There have been studies on hazardous materials like liquefied natural gas (LNG) carriers [4] and tuned liquid dampers (TLDs) [5]. Early research on sloshing started with potential theory and linear wave analysis, focusing on regular geometric models and sloshing problems in freshwater [6-7]. Lu et al. [8] used a Computational Fluid Dynamics-Discrete Element Method (CFD–DEM) model to examine the effect of particle density on sloshing. They found that higher densities increased wave amplitudes, whereas lighter particles provided stronger damping. In addition, synchronising the external excitation frequency with the tank natural frequency improves sloshing suppression due to increased fluid velocity and viscosity effects [8]. Dutta and Laha [9] reported that viscosity had only a minor effect on reducing sloshing pressures inside the tank. Akyildiz and Ünal [10] tested a 3D rectangular model and showed that while viscosity and excitation intensity influenced pressures, the use of baffles effectively reduced liquid motion. The authors also performed numerical studies on sloshing in a rectangular tank with different filling levels.

Chen and Xue [11] used commercial Computational Fluid Dynamics (CFD) software with a six-degree-of-freedom motion platform. They found that in non-resonant conditions, impact pressure scaled with excitation amplitude. As the fill level increased, the sloshing response shifted from soft-spring to stiff-spring behavior, and wave breaking influenced resonance frequency. Faltinsen and Timokha developed a numerical model based on domain decomposition to observe how the filling depth, stiffness ratio and hole positions influenced natural sloshing frequencies [12]. Liu and Lin studied 3D nonlinear sloshing with broken free surfaces using a large eddy simulation (LES) model to account for turbulence effects [13]. Xue

et al. examined different vertical baffle designs and found that changing flow patterns and frequencies could reduce pressure on the tank walls [14].

Kheazzar et al. conducted an experiment with a liquid in a sealed tank subjected to sudden pressure [15]. Zhang et al. studied sloshing in a cubic system using two-phase flow models based on the Navier-Stokes equations under harmonic motion with various partition setups [16]. Jin and Lin investigated the effects of viscosity on sloshing and concluded that the optimal peak pressure occurred near the natural frequency, with small phase shifts due to wave nonlinearity [17]. Oxtoby introduced the semi-implicit VOF method for modeling free surface movements in intense flow situations [18]. Wu et al. [19] applied the fictitious cell method and finite difference schemes to study sloshing in partitioned tanks under pulsed excitations. They later modeled rectangular tanks with vertical perforated baffles under shaking, using the Reynolds-averaged Navier–Stokes (RANS) equations to capture nonlinear waves, air entrapment, and vortices [20]. Nicolici et al. highlighted the importance of combining CFD with finite element analysis (FEA) to predict the pressure, wave amplitude and effects caused by sloshing [21].

The level set (LS) method is a common way to track interfaces in sloshing simulations [22]. To improve mass conservation, Sussman and Puckett combined the VOF and LS methods into the coupled level set volume-of-fluid (CLSVoF) method [23]. Saripilli et al. [24] studied ship sloshing using the finite volume method (FVM) and VoF to capture free surfaces. They showed that fill level strongly affected damping and resonance, underlining sloshing's role in ship motions.

Although many studies have examined sloshing in tanks, fewer have focused on how viscosity and fill level interact to affect dynamic pressure and turbulence kinetic energy in two-phase systems. This study addresses this gap using the VoF method to compare water–air and kerosene–air mixtures at different fill levels in a rectangular tank. The effects of fill level on dynamic pressure and turbulence kinetic energy are analyzed in detail.

2. Theoretical Mathematical Model

Fluid behavior was predicted using the VoF model in Swanson Analysis Systems (ANSYS) Fluent. This method requires two or more immiscible fluids and tracks the "interface" that separates the different fluids. Considering α_q as the volume fraction of fluid q inside the tank, there are three possibilities:

1. $\alpha_q = 0$: The cell is empty of fluid.
2. $\alpha_q = 1$: The cell is completely filled with fluid.
3. $0 < \alpha_q < 1$: The cell contains an interface between fluid and other fluids.

In this study, liquid and gas phases were modeled. The continuity equation was solved for the primary liquid phase, while momentum and energy equations were applied to the mixture. The equations are mentioned below;

The continuity equation;

$$\frac{\partial}{\partial \mathrm{t}}(\alpha\rho) + \nabla \cdot (\alpha\rho\mathbf{u}) = \mathrm{S_m} \tag{1}$$

The momentum equation is;

$$\frac{\partial}{\partial t}(\rho u) + \nabla \cdot (\rho u u) = -\nabla p + \nabla \cdot [\mu(\nabla u + \nabla u^T)] + \rho g + S_{CSF} \quad (2)$$

Here, p represents local pressure, μ is dynamic viscosity and g denotes gravitational force.

Surface tension arises from uneven molecular forces at liquid–vapor interfaces. It pulls molecules inward, minimizing the energy of bubbles or droplets, and influences bubble formation and liquid adhesion to solids. The Continuum Surface Force (S_{CSF}) model accounts for these effects by appending a contributing factor (S_{CSF}) to the momentum equation. This improves the accuracy of fluid dynamics modeling.

2.1. Volume Fraction Equation

Volume separators separate multiple phases in a closed domain by gravity, using density differences between phases. To track the interface in volume separators, the continuity equations between the phases must be solved. The continuity equation for fluid q is as follows:

$$\frac{1}{\rho_q}[\frac{\partial}{\partial t}(\alpha_q \rho_q) + \nabla \cdot (\alpha_q \rho_q \vec{V}) = S_{\alpha q} + \sum_{p=1}^{n} (\dot{m}_{pq} - \dot{m}_{qp})] \quad (3)$$

$\dot{m}_{pq}$ represents mass transfer from phase p to phase q. Here, $S_{\alpha q}$ is typically zero, but can be defined by the user to represent a mass exchange between the phases. This term allows modeling of phase changes or other processes involving interphase mass exchange. To solve the volume fraction equation, explicit time discretization is applied;

2.2. Explicit Scheme

$$\frac{\alpha_q^{n+1}\rho_q^{n+1} - \alpha_q^n \rho_q^n}{\Delta t} V + \sum_f (\rho_q U_f^n \alpha_{q,f}^n) = [S_{\alpha q} + \sum_{p=1}^{n} (\dot{m}_{pq} - \dot{m}_{qp})]V \quad (4)$$

$n + 1$ = Index for the new (current) time step
n = Index for the previous time step
$\alpha_{q,f}$ = Volume fraction of phase q at the face at time step n
V = Volume of the cell
U_f = Volume flux (mass flux)

3. Numerical Model

Sloshing was induced by applying an acceleration of 3.75 m/s² to the tank for 3 seconds. For simplicity, the sloshing motion was analyzed in two dimensions. The model for turbulence used in this project is the Shear Stress Transport (SST) k-ω turbulence model, which is based on the Reynolds-Averaged Differential Stokes equations also known as RANS. The SST k–ω model combines the advantages of the standard k–ε and k–ω models, using k–ω near walls and k–ε in the far field. It effectively captures transient, wall-bounded flow phenomena such as sloshing

and can also be applied to unsteady boundary flows. This is due to its higher accuracy in predicting the separation of flows and intensities of turbulence around solid surfaces. ANSYS Fluent was chosen for its robustness and reliability in simulating multiphase flows with free-surface deformation. A time step of 0.002 s was used in the simulations. This also is the value of a necessary minimum which allows you to predict the rapid changes of the fluid motion in the initial phase of sloshing properly.

3.1. Tank Configuration

A 2D tank with dimensions of 5.5 m × 1.75 m was selected. For the parametric study, liquid heights were set at 0.875 m and 1.3125 m in the cross-section.

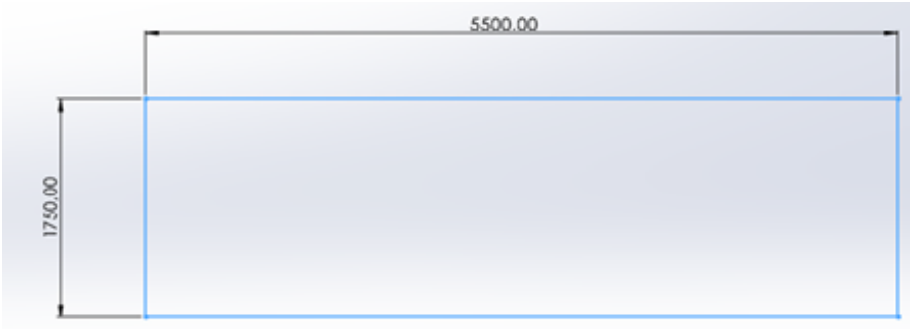

Fig.1. 2D Model Dimensions

3.2. Mesh

The geometry was meshed with 5,920 hexahedral elements of 4 mm size. The hexahedral mesh structure closely followed fluid motion, reducing numerical diffusion and improving multiphase sloshing accuracy. The meshed geometry is shown in Fig. 2. To evaluate mesh resolution effects, a mesh independence study was conducted. Three different mesh sizes were tested: 20 mm, 30 mm and 40 mm. The maximum dynamic pressure and turbulence kinetic energy values were recorded for every case. Differences between 30 mm and 40 mm meshes were negligible (<2%). The 20 mm mesh provided finer detail but required significantly more computation time. Besides the above considerations, the 40 mm mesh was chosen as the preferred one among the meshes.

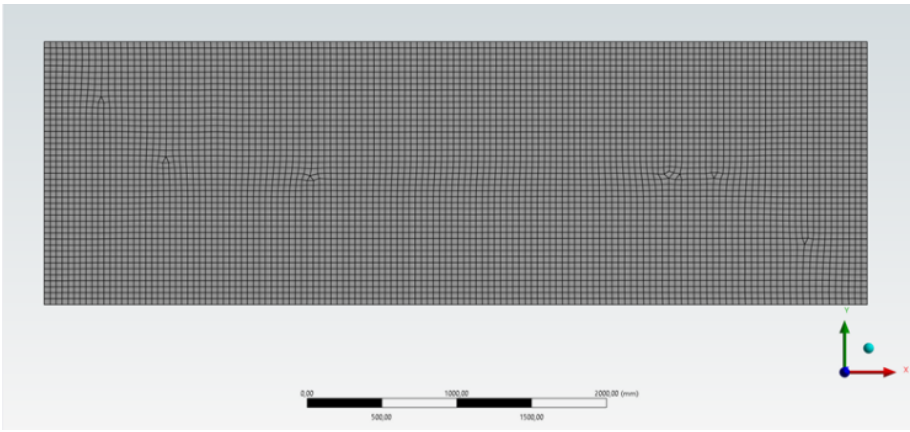

Fig. 2. Mesh View

The distinguishing properties of the fluids used are provided in the table below;

Table 1. Fluid Properties

Fluid	Density (kg/m^3)	Viscosity (kg/ms)
Air	1.225	1.789e-5
Water	998.2	0.00100
Kerosene	800	0.0024

4. Results

The analyses examined sloshing of kerosene–air and water–air mixtures at 50% and 75% fill levels. Results were evaluated in terms of dynamic pressure on tank walls and turbulence kinetic energy (TKE), and comparisons were made between the fluids.

4.1. Dynamic Pressure

Figure 1 is drawing a comparison of the dynamic pressure as a function of time for all the models graphically. This is a visual representation that records the effect of pressure applied to the tank walls during the sloshing motion. Dynamic pressure is proportional to fluid velocity and density. Although kerosene is less dense than water, its higher viscosity produced greater wall pressures. This higher viscosity increased flow resistance, intensifying momentum transfer to the walls and resulting in higher pressures than in water models. There is an impact of viscous damping on the energy distribution in the flow thus establishing the power and the duration of pressure peaks.

As shown in Fig. 3, both fluids peaked within the first second due to sudden acceleration. Pressures then decayed as energy dissipated, with oscillations nearly vanishing by 5 s. The following observations were made upon checking through the result graphs and simulation outcomes;

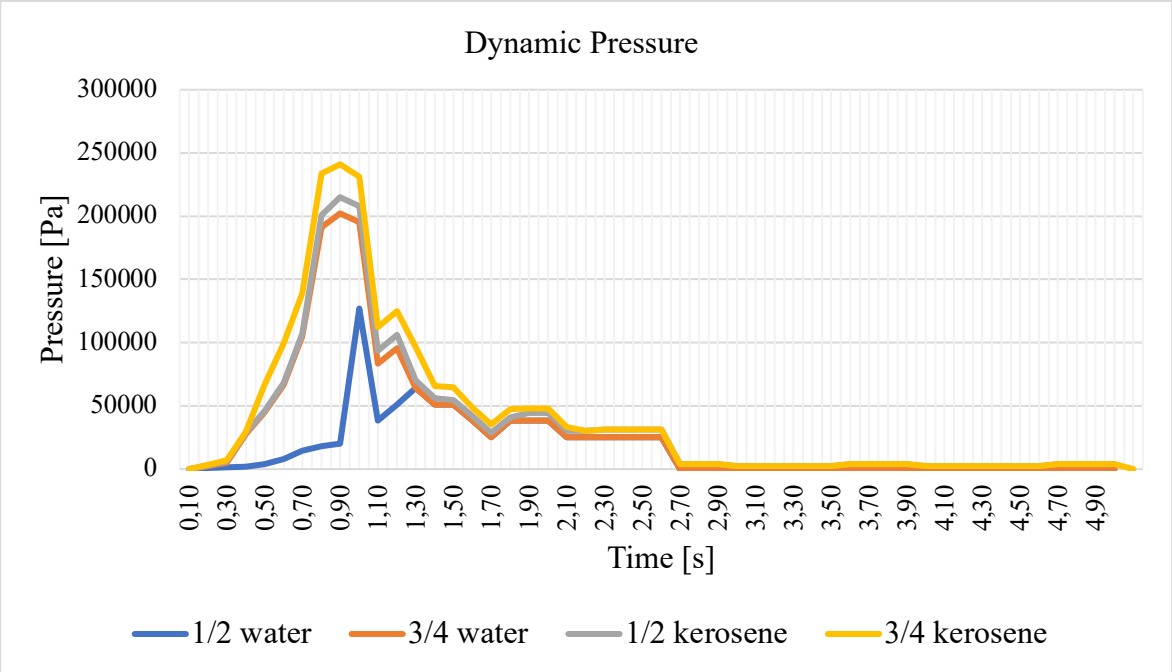

Fig. 3. Dynamic Pressure

- ✓ The highest pressure measured was in the 75% the kerosene-filled model, with about 2.3 kPa being the dynamic pressure developed. On the other hand, in the 50% kerosene-filled model, this value was found to be about 1.8 kPa.

- ✓ The dynamic pressure was lower in the water-filled models. In the 50% water-filled model, the pressure was about 1.27 kPa, while in the 75% water-filled model, it was about 1.5 kPa. Hence, lower water pressure was the outcome compared to kerosene.

- ✓ An increase in the fill level resulted in higher dynamic pressures for all fluids by limiting the sloshing motion. This is, actually, as the fill level increases the mass of the fluid moves more hence, the pressure being exerted on the tank walls is more.

- ✓ In the kerosene-filled models, the pressure was 20% to 30% greater in the water-filled models. This is due to kerosene's high viscosity, which is thus more responsible for the higher pressure due to the wall taking more the load which is greater pressure.

4.2. Turbulence Kinetic Energy

Figure 4 shows TKE over time. All models exhibited synchronized motion under the same acceleration. According to the simulation results, the turbulence kinetic energy reached its maximum level in the first second when sloshing began and then gradually decreased as the fluid's energy dissipated over time. This indicates that the sloshing motion initially had high energy, but this energy diminished as time passed. Upon reviewing the result graphs and simulation outcomes, the following points are noteworthy:

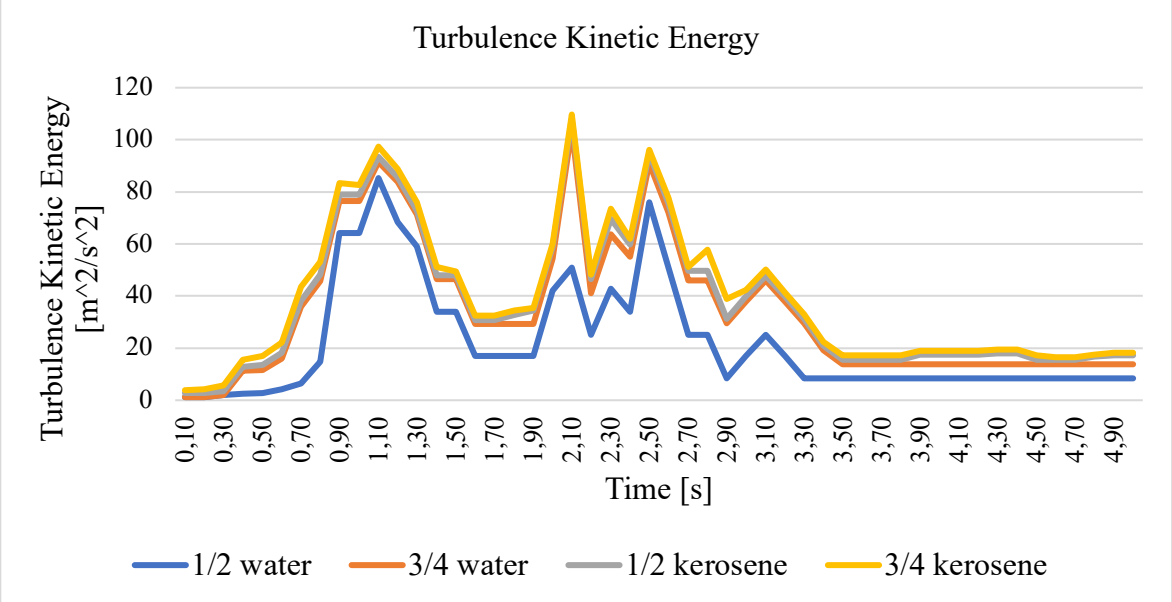

Fig. 4. Turbulence Kinetic Energy

- ✓ When the liquid started to slosh, there was a very quick minute increase in turbulence kinetic energy but soon after it reduced when the fluid gradually lost its sloshing energy until it reached an almost steady value.

- ✓ The maximum TKE value was registered in the 75% kerosene-filled geometry model, with the obtained value of a maximum TKE of around 0.08 m^2/s^2. However, in the case of the water-filled models, the TKE of the models showed lower values at the end of the experiments.

✓ The largest TKE value was around 0.05 m^2/s^2 in the 50% water-filled model and nearly 0.06 m^2/s^2 in the 75% water-filled model as it remained the same even with an increase in the volume of liquid in the models.

In general, it is observed that TKE values are higher in kerosene-filled models compared to water-filled models. The viscosity of kerosene (60 cSt-285 cSt) is higher than water and the former can store more energy per amplitude period, providing a rise in the observed average velocity of the movement. Greater viscosity increased drag and velocity fluctuations, leading to higher TKE. Both the volume fraction images of the respective models can be viewed at the bottom. The matching images of the same amount of kerosene and water are shown and we can see that the viscosity of the fluid has a positive effect on the sloshing. Moreover, opposing the initial assumption, the positive correlation between the levels of kerosene and water was found in the models.

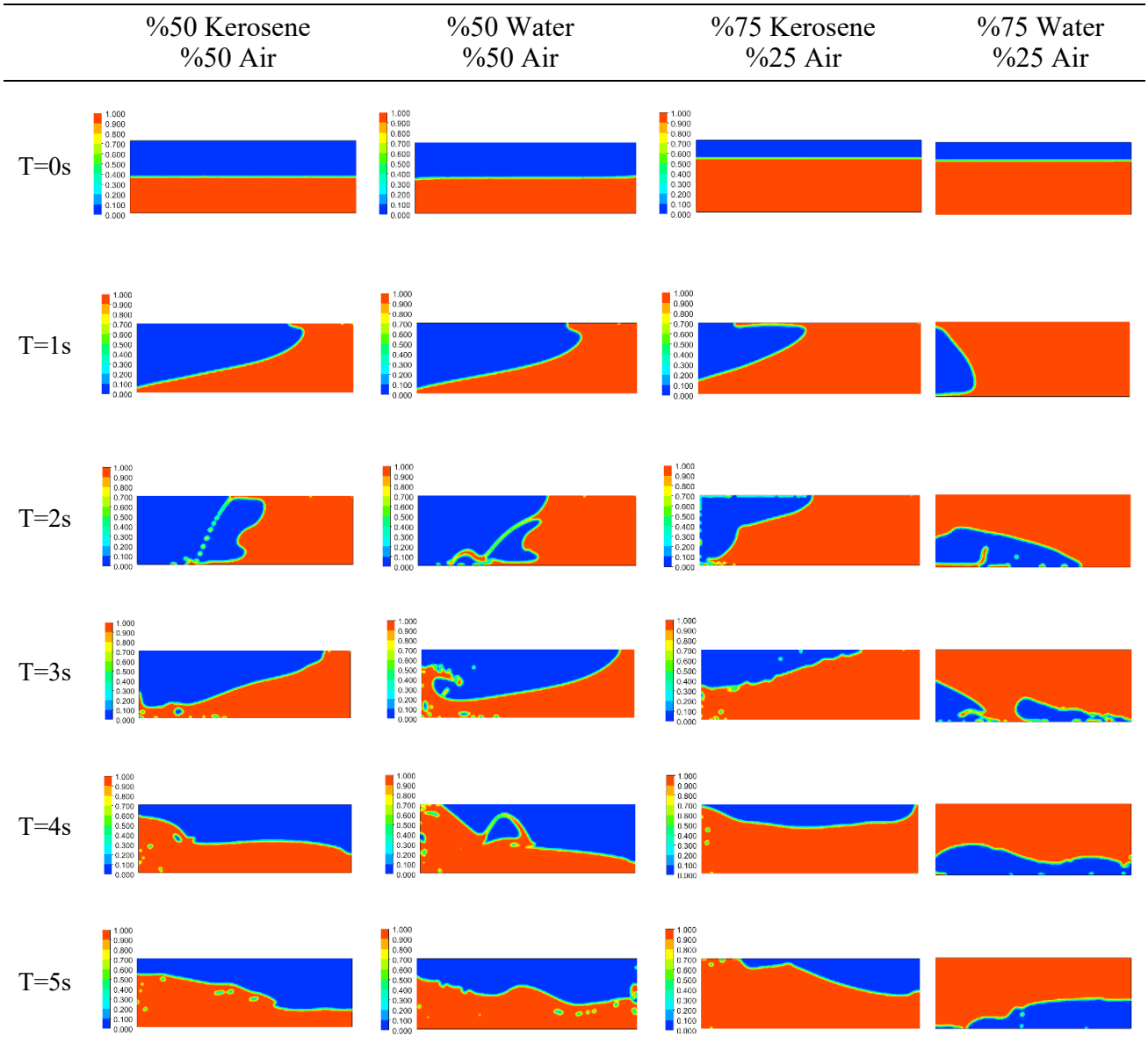

Fig. 5. Sloshing Simulations

5. Conclusion

The study is devoted to the issue of liquefied kerosene and water-air sloshing in a rectangular tank using the VoF model. The main focus was on the dynamic pressure and turbulence kinetic energy, depending on the fluid type, fill level and viscosity. The main findings in brief are:

- ✓ The maximum pressure was observed in the 75% kerosene-filled model, which was about 2.3 kPa. On the other hand, the 50% kerosene-filled model only produced a low pressure of around 1.8 kPa. Water-filled models had lower dynamic pressure values with 1.27 kPa and 1.5 kPa in the 50% and 75% water-filled models, respectively. This shows that kerosene, due to the higher viscosity, is the one that generates higher pressure on the tank walls.

- ✓ Turbulence kinetic energy was higher in the kerosene-filled models than in the water-filled models, too. The highest TKE was observed in the 75% kerosene-filled model, which was in the range of 0.08 m^2/s^2, whereas the 50% kerosene model reached about 0.07 m^2/s^2. The water-filled models had the TKE values less, with a maximum of 0.05 m^2/s^2 in the 50% model and 0.06 m^2/s^2 in the 75% model.

- ✓ The discrepancy in both dynamic pressure and TKE can be ascribed to the higher viscosity of kerosene, which results in the resistance to the movement of the fluid during sloshing. A higher viscosity causes more energy dissipation and velocity fluctuation, which is why higher pressure and turbulence happen closer to the walls of the tank.

- ✓ Moreover, the analysis called attention to the fact that pushing the fill level upward led to a more significant Dynamic pressure and TKE for both liquids. The resultant conditions from the increase in liquid mass, for the pressure and turbulence in the tank to go up due to higher fluid motion has been thereby produced.

As a result, the type of fluid, its viscosity and the fill level are three primary factors that determine the dynamic behavior in tanks. It is finally summarized that implementations of kerosene are the most probable to bring about increased dynamic pressure and to create higher turbulence inside the tank, because it is a more viscous fluid compared to water. These are the parameters through which new fluid-carrying tanks are designed, which ensure strength and high performance, especially during the transportation of highly viscous or hazardous fluids.

Author Contribution

Furkan Tan: Conceived and designed the analysis, Wrote the paper, Prepared the paper for publication.

Hamid Orhun Tur: Conducted a literature review, designed the analysis, verified the theories and methods.

References

[1] Ibrahim, R.A., Liquid Sloshing Dynamics. Theory and Applications, *Cambridge University Press*, 2005.

[2] Cai, Z., Topa, A., Djukic, L. P., Herath, M. T., & Pearce, G. M., Evaluation of rigid body force in liquid sloshing problems of a partially filled tank: Traditional CFD/SPH/ALE comparative study. Ocean Engineering, 236, 109556, 2021.

[3] Gao, J., Hou, L., Liu, Y., & Shi, H., Influences of bragg reflection on harbor resonance triggered by irregular wave groups. Ocean Engineering, 305, 117941, 2024.

[4] Wang, X., Makoto, A., A study on coupling effect between seakeeping and sloshing for membrane-type LNG carrier. *International Journal of Offshore & Polar Engineering*, 21(04), 2011.

[5] Chen, Y., Wei-Shien, H., Wen-Huai, T., Nonlinear dynamic characteristics of rectangular and cylindrical TLDs. *Journal of Engineering Mechanics*, 144(9), 06018004, 2018.

[6] Graham ,W.C., Severe injuries to the hand. *Journal Iowa State Medical Society*, 381-382, 1951.

[7] Housner, G.W., Dynamic pressures on accelerated fluid containers. *Bulletin of the Seismological Society of America*, 47(1), 15–35, 1957.

[8] Lu, L., Zhu, R., Ji, C., Guo, J., Lyu, F., & Xu, S., Influence of solid particles in liquid tank on sloshing behavior based on CFD-DEM coupling method. Ocean Engineering, 312,119068, 2024.

[9] Dutta, S., Laha, M.K., Analysis of the small amplitude sloshing of a liquid in a rigid container of arbitrary shape using a low-order boundary element method. *International Journal for Numerical Methods in Engineering*, 47(9), 1633-1648, 2000.

[10] Akyildiz, H., Ünal, E., Experimental investigation of pressure distribution on a rectangular tank due to the liquid sloshing. *Ocean Engineering*, 1503-1516, 2005.

[11] Chen, Y., Xue, M.A., Numerical Simulation of Liquid Sloshing with Different Filling Levels Using OpenFOAM and Experimental Validation. *Water*, 10(12), 1752, 2018.

[12] Faltinsen, O.M., Timokha, A.N., Natural sloshing frequencies and modes in a rectangular tank with a slat-type screen. *Journal of Sound and Vibration*, 1490-1503, 2011.

[13] Liu, D., Lin, P.A., Numerical study of three-dimensional liquid sloshing in tanks. *Journal of Computational physics*, 227,3921–3939, 2008.

[14] Xue, M.A., Experimental study on vertical baffles of different configurations in suppressing sloshing pressure. *Ocean Engineering*, 136, 178-189, 2017.

[15] Khezzar, L., Abdennour, S., Afshin, G., Water sloshing in rectangular tanks – an experimental investigation and numerical simulation. *International Journal of Engineering*, 3(2),174-184, 2009.

[16] Jin, X., Lin, P., Viscous effects on liquid sloshing under external excitations. *Ocean Engineering*, 171, 695-707, 2019.

[17] Oxtoby, O.F., Malan, A.G., Heyns, J.A., A computationally efficient 3D finite-volume scheme for violent liquid–gas sloshing. *International Journal for Numerical Methods in Fluids*, 79, 306–321, 2015.

[18] Wu, C.H., Faltinsen, O.M., Chen, B.F., Numerical study of sloshing liquid in tanks with baffles by time-independent finite difference and fictitious cell method. *Computers & fluids*, 63, 9-26, 2012.

[19] Poguluri, S.K., Il-Hyoung, C., Mitigation of liquid sloshing in a rectangular tank due to slotted porous screen. *Proceedings of the Institution of Mechanical Engineers, Part M: Journal of Engineering for the Maritime Environment*, 686-698, 2020.

[20] Nicolici, S., Bilegan, R.M., Fluid structure interaction modeling of liquid sloshing phenomena in flexible tanks. *International Journal of Nuclear Engineering and Design*, 258, 51-56, 2013.

[21] Benmasaoud, B., Essaouini, H., Hamydy, A., Lhassane Lahlaouti, M., Sloshing analysis of a two-layered fluid in a tank with baffles using Level Set Method. International Review of Applied Sciences and Engineering, 2024.

[22] Sussman, M., Peter, S., Stanley, O., A level set approach for computing solutions to incompressible two-phase flow. *Journal of Computational Physics*, 114(1),146-159,1994.

[23] Sussman, M., Elbridge, G.P., A coupled level set and volume-of-fluid method for computing 3D and axisymmetric incompressible two-phase flows. *Journal of Computational Physics*, 162(2), 301-337, 2000.

[24] Saripilli, J.R., Debabrata, S., Numerical studies on effects of slosh coupling on ship motions and derived slosh loads. *Applied Ocean Research*, 76, 71-87, 2018.